Microstructural Modification of Sn-Bi and Sn-Bi-Al Immiscible Alloys by Shearing

Z. Cassinath[1], Z. Li[1], S. Sridhar[1,2], A. Das[3], H. R. Kotadia[1*]

[1]Warwick Manufacturing Group, University of Warwick, Coventry CV4 7AL, UK

[2]Kroll Institute for Extractive Metallurgy, Colorado School of Mines, 1500 Illinois St. Golden, CO 80401, USA

[3]College of Engineering, Swansea University, Bay Campus, Fabian Way, Swansea SA1 8EN, UK.

[*]e-mail: H.Kotadia@warwick.ac.uk

Abstract: Sn–20 wt-%Bi and immiscible Sn–20 wt-%Bi–1 wt-%Al alloys were used to understand the effect of high-intensity shearing on microstructural refinement. Novel ACME (Axial Centrifugal Metal Expeller) shearing device, based on axial compressor and rotor–stator mechanism to generate high shear rate and intense turbulence, was used to condition the melts prior to solidification. Microstructure in the Sn–Bi alloy deviated from dendritic grains with coarse eutectic pockets under conventional solidification to compact grains with well-dispersed eutectic under semisolid-state shearing. Decreasing the shearing temperature and increasing shearing time increased the globularity of grains. Following shearing, remnant liquid solidified into fine grain structure. In the immiscible Sn–Bi–Al alloy, shearing produced uniform dispersion of refined Al-rich particles in Sn-rich matrix as opposed to severe segregation under conventional solidification. The primary effect of shearing appears to originate from the thermo-solutal homogenisation of the melt and its effect on interface stability during solidification.

Keywords*: Solidification, microstructure, semisolid, Sn alloys, immiscible, coarsening, grain refinement, melt shearing*

Introduction

Phase transformation, microstructure evolution and associated defect formation during solidification are critical to the properties of metallic materials [1, 2]. Therefore, the microstructure evolution of alloys during solidification has attracted continuous attention in academia and industry [3]. The microstructure of an alloy is of significant importance, since many of its mechanical properties are directly related to the size, shape and distribution of the various phases. It is well known that the production of a fine-grained equiaxed structure leads to a substantial improvement in the quality of the casting and a minimises cracking. Cast alloy microstructures can be modified through three major approaches; (i) chemical grain refining by adding efficient nucleation sites and restricting grain growth e.g., Al-5Ti-1B grain refiner used for Al alloys [4] and Zr for Mg alloys [5], (ii) physical grain refining by producing a vigorous forced convection in the melt during freezing leading to substantial grain refinement e.g., use of ultrasonication [6-9], electromagnetic field [10], intensive shearing [11-13] and (iii) controlling solidification parameters such as cooling rate and melt superheat etc.

Chemical grain refining is one of the most utilised industrial techniques as it is easily applicable and does not require any specific training and additional resources for high-volume manufacturing. However, chemical grain refinement is known to be sensitive to poisoning alloying additions e.g., Al-Ti-B grain refiner is not beneficial when Al-alloys have higher Si content [4], and similarly, Zr is ineffective in Mg-alloys containing Al [14]. In addition, chemical grain refiners are not capable of refining other phases in alloys such as eutectic and intermetallics. While eutectic modifiers, such as Sr, can refine and modify the eutectic in Al-Si alloys, primary grain structure cannot be refined by such additions. As an alternative to the chemical approach, physical means have been explored for microstructural

modification of various aluminium and magnesium cast alloys. Each of these physical techniques have been met with varying degrees of success.

Limitations of the chemical approach can be addressed by physical microstructure modification. These include applicability to a wider range of alloy systems and phases, environmental sustainability, cost effectiveness, no fading or poisoning effect, and benefits to mechanical strength and corrosion properties. Physical grain refining has been applied at various stages during solidification. It can broadly be classified as processes applied above or below the liquidus temperature. When processed above the liquidus, benefits include increased heterogeneous nucleation due to dispersion of oxide particles as nucleation sites [7, 15, 16] and a uniform chemical composition throughout the liquid. Critical reviews published by Flemings [17] and Fan [11] covers processing below the liquidus, also known as semi-solid metal (SSM) processing, where solid-liquid slurry is treated to achieve a physically induced grain refinement through fragmentation and coarsening. Initial work by Flemings and co-workers [17] involved shearing solidifying liquid using a simple "propeller". Subsequent work by Fan and co-workers [11] involved a specially-designed twin-screw instrument in order to provide intense shearing to the semisolid slurry. Twin-screw device [18] has shown microstructural refinement of Al and Mg alloys when slurry with less than 30 wt.% of solid fraction is sheared. However, twin-screw is difficult to incorporate into casting processes mainly due to the size, compatibility and operational complexities. In order to overcome these challenges, new instruments have been devolved based on rotor–stator shearing mechanism [19]. In the present research, ACME (Axial Centrifugal Metal Expeller) [18, 19] shearing device working on the same principle as the rotor-stator instrument is used. The ACME device provides high intensity shearing through blade and shaft design as well as adds flexibilities in terms of processing Metal Metrix Composite (MMC), pumping liquid etc.

A variety of mechanisms are thought to contribute to this refinement e.g., physical detachment of secondary dendritic arms from primary arm, remelting of dendritic arms at their roots and formation of rosettes under coarsening of dendrites through forced convection [11, 17]. In this way, a uniform and predominantly non-dendritic microstructure is achieved throughout the ingot without any chemical segregation. Mullis [20] showed by computer simulation that dendritic arms bend into the flow due to thermo-solutal convection, resulting in rosette morphology.

In the present research, the β – Sn grains, Bi eutectic and Al-rich phase refinement and distribution under melt shearing have been explained based on the effect of intensive shearing and the nature of fluid flow. The β – Sn grain morphological evolution is discussed from the effect of convection on the diffusion boundary geometry around the growing solid–liquid interface as studied by Das et al. [3] through Monte-Carlo simulation. All these finding from Sn-Bi alloys have important implications for the understanding of cast Al-Si alloy semi-solid metal behaviour and its rheological properties.

Experimental procedure

Material preparation: Model Sn-Bi alloy was used in this study as a low temperature analogue to common casting alloys involving a microstructure consisting of primary grains surrounded by grain-boundary eutectic. The immiscible Sn-Bi-Al alloy was chosen to demonstrate the effectiveness of shearing in alloy systems not amenable to conventional casting. The two selected alloys, Sn-20Bi and Sn-20Bi-1Al (all composition expressed in wt.%), were prepared from commercially pure Sn, Bi and Al in a clay-graphite crucible using an electric resistance furnace. For each batch of experiments, around 2–3 kg of pure metal or alloy was melted and homogenised for 1 h at ~ 50 °C above the liquidus (for Sn-Bi) and critical temperature (Sn-Bi-Al), T_c (where both L′ and L′′ liquids are completely miscible). A

schematic Sn-Bi phase diagram is shown in Fig. 1, which defines some of the processing parameters.

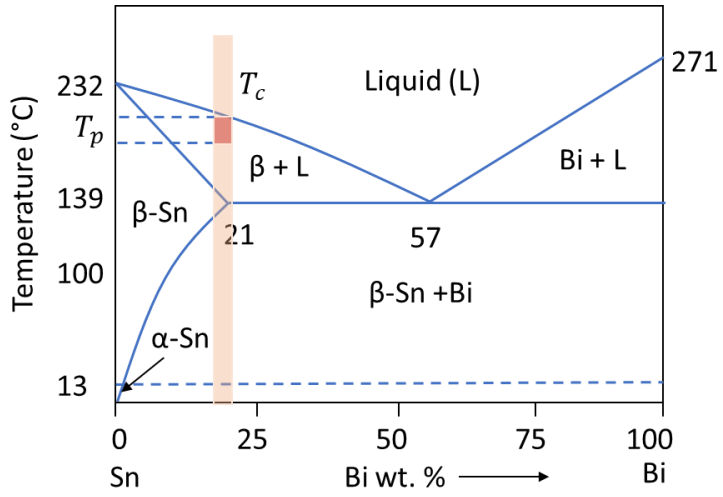

Fig. 1. A schematic Sn-Bi phase diagram illustrating relevant terminology and processing temperature.

ACME unit: The ACME unit is designed to refine microstructure and distribute particles and various phases for enhanced mechanical and chemical properties. The ACME instrument, designed by Cassinath [18, 19], comprises a shaft with several rotor blades, which is driven by a motor. Each stator is fixed into the walls of the barrel and sits in slots. Figure 2 shows the assembly of the ACME instrument. The important parameters for this instrument include the sequence of a holding/reservoir stage and the vertically alternating arrangements of stator and rotor stages. Powerful and dispersive mixing at a very fine level for the flow inside the ACME unit can be achieved by the high shear rate and high intensity of turbulence generated inside the unit. The highly intensive shear also homogenises the melt temperature and chemical composition along with even dispersion of nucleation sites and preformed particles in the melt volume.

This instrument can be used in various ways to suit established casting process e.g., direct-chill (DC) casting and high-pressure die-casting (HPDC) etc. In the present study, it was adapted as a submersible device. Before the experiments, the ACME unit was heated to the semisolid region (processing temperature, T_p) of the alloy to be used. The ACME unit was submerged into the crucible holding the melt and the system was homogenised at T_p.

The required rotational speed was applied at three different T_p (all below the liquidus temperature) to understand the effect of shearing at various solid fraction of primary β – Sn being present in the semisolid slurry. In the immiscible system, the ACME unit was switched on well above T_c to avoid liquid phase separation before shearing commenced. In each case, the conditioned melt was cast in alumina moulds after shearing. For comparison, solidification experiments were conducted without shearing under natural cooling conditions.

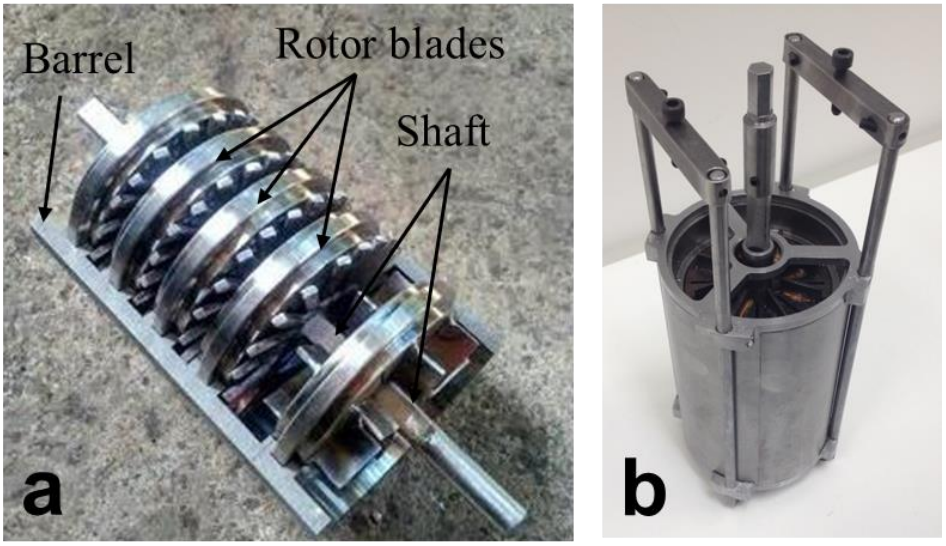

Fig. 2. ACME unit (a) unassembled unit and (b) assembled unit used for shearing. Assembled unit was immersed into liquid crucible to achieved desired shearing on semi-solid slurry.

Microscopy and Quantitative Metallography: Samples for microstructural examination were machined from the castings and cold mounted using epoxy mounting resins & hardeners. The mounted specimens were ground using standard metallographic techniques with SiC abrasive paper and polished with a 0.25-μm silica mastermet suspension by Buehler Ltd. The microstructures were observed following etching with 3% concentrated HNO_3 for optical microscopy and without etching for Scanning Electron Microscopy (SEM). SEM work was carried out on a Hitachi TM3030 Plus Desktop SEM and on a Zeiss Sigma Field Emission Gun (FEG)-SEM equipped with Oxford Instruments EBSD and EDS detectors. Quantitative analysis was carried out using an automated Zeiss AxioVision image analysis software where grain size calculation was conducted using the linear intercept method.

Results

Primary β – Sn grain refinement in Sn-Bi alloy

In order to assess the effect of high-intensity shearing on primary *β*–Sn grain structure, Sn-Bi alloys were processed with and without shearing. The microstructures observed in material processed under different conditions are presented in Fig. 3. The corresponding processing conditions and microstructural features are summarised in Table 1. Without shearing, the base microstructure consists of well-developed dendritic grains (Fig. 3a and Fig. 4a) with an average grain size ranging between 500 to 1000 μm in various regions of the solidified ingot. In contrast, complete conversion to non-dendritic grain structure is observed after intense shearing (Fig. 3c) with an average grain size varying from ~67 ± 28 μm. In addition, the microstructure revealed two distinct sizes of *β* – Sn grains. The larger of which ranged between 150 to 250 μm, while the smaller grains were approximately 34 μm in average size. In order to ensure reproducibility of the observed results, shearing experiments were repeated several times, all resulting in similar grain size distribution in the solidified ingots. After

treating the semisolid slurry under high shear rate and high intensity turbulence for 1 to 15 minutes, as shown in Fig. 3c and Fig. 4b, the morphology of β – Sn grains was found to be spherical even at the early stage of solidification. To understand growth behaviour of the primary phase, the slurry was sheared at different temperature from 195 – 230 °C. The experimental results indicate that an intermediary rosette microstructure is achieved when a sample is sheared at higher temperature for less than one minute (Fig. 3b). It is concluded that reducing shearing temperature and increasing shearing time increases the sphericity of primary β – Sn grains. In addition to that, viscosity of the slurry was also observed to reduce through intensive shearing under isothermal conditions that follows the thixotropic behaviour usually shown by semisolid slurries under shear [11].

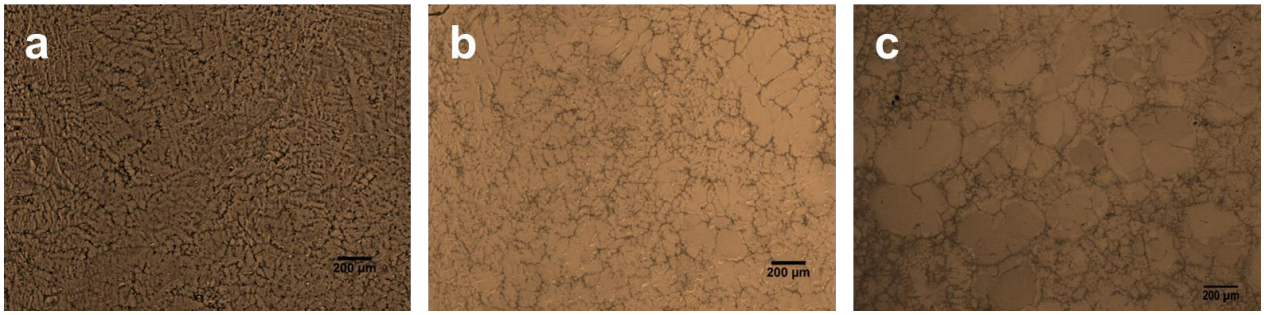

Fig. 3. Morphological transition of Sn-20Bi alloy microstructure from (a) dendritic to (c) globular via (b) rosette. (a) is without shear and cast at 230 °C, (b) sheared less than 1 minute at 205 °C, and (c) sheared for 5 minute (total) at 195 °C.

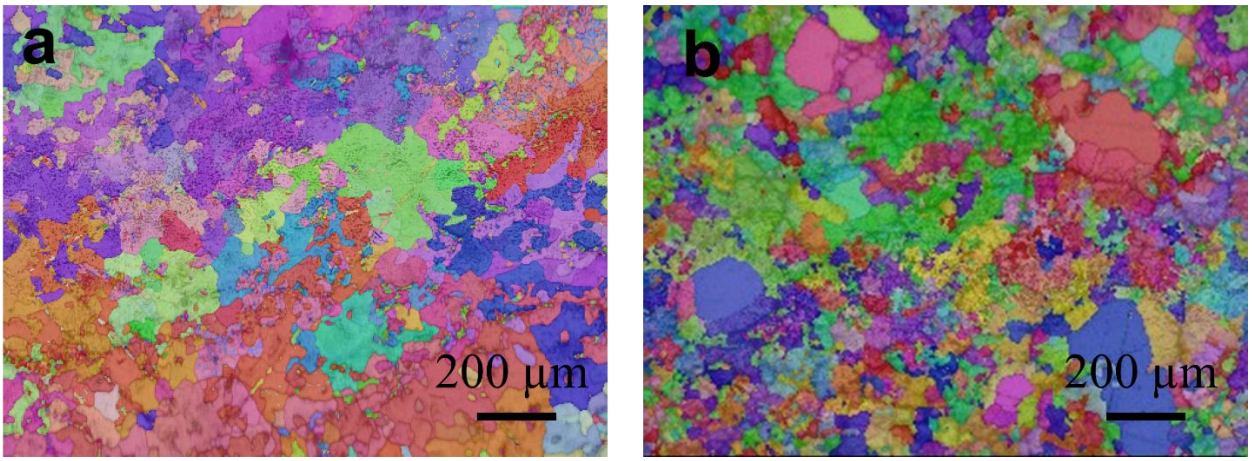

Fig. 4. EBSD image of Sn-20Bi alloy microstructure (a) without shearing and (b) sheared. After shearing dendritic grains transformed to fine and globular grains.

Table 1. Summary of the processing conditions and the microstructural features of the Sn-Bi alloy

Condition	Temperature (°C)	Grain morphology	Sphericity	Grain size range (µm)
Without sheared	230	Dendritic	-	500 – 1000
Sheared	205	Rosette	0.80	500
Sheared	200	Spherical	0.91	34-250
Sheared	195	Spherical	0.92	34-250

Eutectic distribution in Sn-Bi alloy

Fig. 5 shows the microstructural distribution of the eutectic produced at the last stage of solidification ($L \rightarrow \beta - \mathrm{Sn} + \mathrm{L} \rightarrow \beta - \mathrm{Sn} + \mathrm{eutectic}$), which had a very fine laminar morphology with a spacing less than 1µm. The fine eutectic forms a continuous network delineating the primary particles. In the absence of melt shearing, the eutectic formed isolated

and segregated pockets between the primary *β*–Sn grains distributed randomly in the microstructure (Fig. 5a and c). The micrographs from sheared samples revealed that solidification under intensive shear could alter the eutectic distribution within the matrix. The eutectic was evenly distributed throughout the matrix forming a continuous network as shown in Fig. 5b and d. This is primarily due to the refined non-dendritic grain morphology of the *β* – Sn that allowed even distribution of the remaining liquid in the microstructure promoting a connected and well-distributed intergranular eutectic.

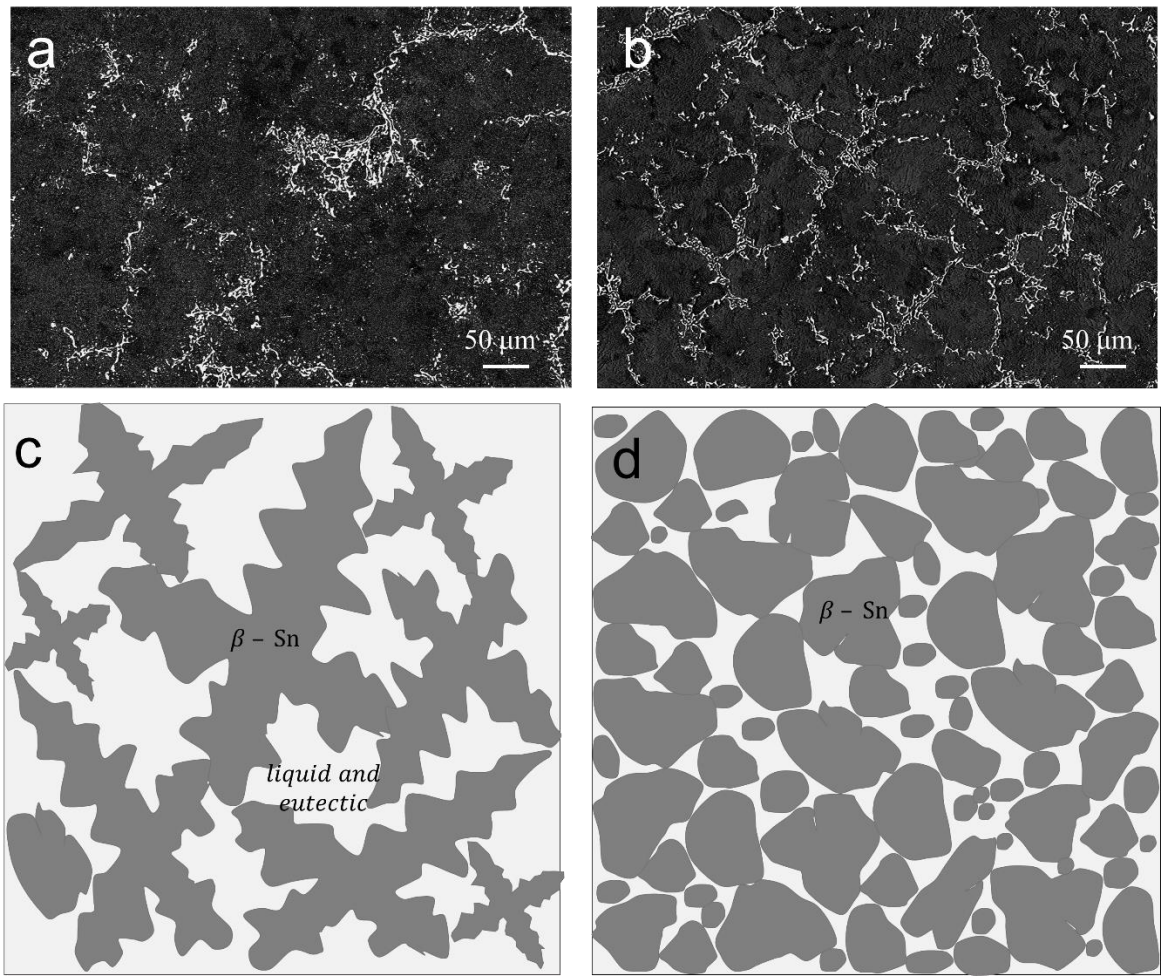

Fig. 5. Backscatter SEM image of Sn-20Bi alloy (a) without shearing and (b) sheared. White phase in the microstructure represents eutectic- Bi. Schematic illustration of primary-grains and eutectic distribution in non-sheared (c) and sheared (d) samples; sheared sample shows well-distributed eutectic in the matrix.

Distribution of Al-rich phase in immiscible alloys

The most significant difference observed between the microstructures in the absence and presence of shearing (Fig. 6) is that a homogeneous dispersion of the Al-rich phase within the Sn-Bi matrix is achieved only under shearing. Additionally, complete separation of two liquids (Sn-rich and Al-rich) was also noticed in some unsheared samples but prevented under shearing. The distribution of the hard particles (black in the SEM image Fig. 6) is uniform under shearing. This implies that shearing is effective in dispersing and distributing the separated liquids, and accordingly, the soft and hard phases in the microstructure of immiscible metallic systems. However, Kotadia [13, 21] has noted that increasing the volume fraction of soft or hard phase reduces distance between the liquid droplets and creates agglomeration of phases. It is worth noting that the dispersion effect of shearing is lost on holding following shearing leading to further coagulation and segregation of the immiscible phases. Accordingly, it is important that samples are cast as quickly as possible to retain the benefits of shearing and prevent phase coagulation.

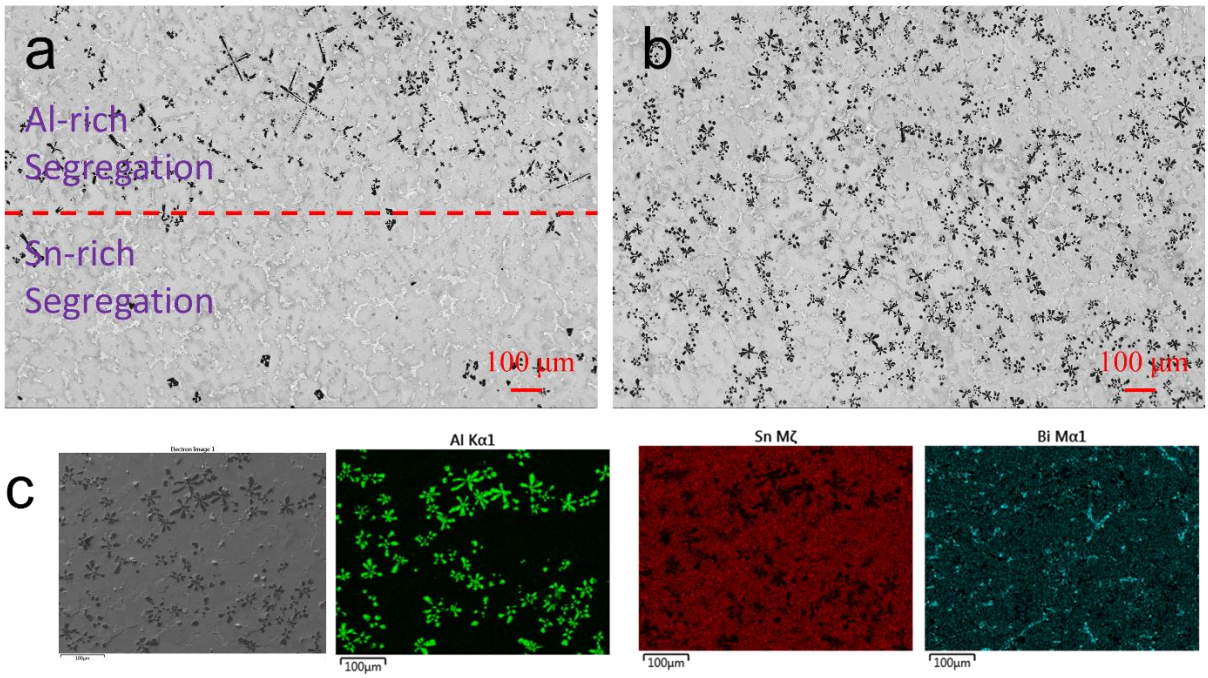

Fig. 6. Secondary electron SEM image of Sn-20Bi-1Al immiscible alloy (a) without shear and (b) sheared and (c) EDS map of sheared sample. Comparatively uniform distribution of Al-rich phase within the matrix is achieved through melt shearing.

Discussion

Effect of shearing on the morphology and distribution of primary β – Sn and eutectic

The exact effect of intensive shearing on microstructure modification has not been irrefutably established. Two major mechanisms are proposed in the literature (i) enhanced heterogeneous nucleation and (ii) particle fragmentation. According to the enhanced heterogeneous nucleation theory, the forced wetting of insoluble inclusions occurs under fluid flow and convection that leads to more substrates for grain nucleation [22]. Experimental reseach on wetting of MgO and $MgAl_2O_4$ oxide particles in Al–Mg alloy melt has been observed to support this [15]. On the other hand, dendritic fragmentation through fluid flow is well-received and accepted for microstructure refinement.

One needs to consider the application regime of shearing in understanding its effect on microstructure modification. Shearing entirely above the liquidus eliminates possible dendrite fragmentation as solidification commences after shearing, and any observed refinement can be attributed to enhanced nucleation effect. If the shearing is performed well above the liquidus, forced wetting of natural substrates may explain observed refinement. However, previous experimental results [23] show minor refinement effect under such conditions illustrating that enhanced nucleation doesn't entirely originate from forced wetting of substrates. Shearing near the liquidus promotes temperature homogenisation of the entire melt volume that may lead to nucleation in the bulk melt and survival of nuclei in conjunction with forced wetting of nucleants. For shearing below the liquidus, dendrite fragmentation, enhanced nucleation or a combination of both mechanisms may be operating. In the present research, we have applied shearing close to the liquidus temperature or in the semisolid region.

Shearing in semisolid state was observed to create microstructure modification compared to conventional castings. As opposed to the dendritic microstructure formed under conventionally solidification conditions, the microstructure of the alloys processed by ACME unit can have compact particles, rosettes or coarsened dendrites. The shearing conditions during processing and subsequent solidification after processing are the key parameters to control the microstructure. This is indicative of progressive reduction of surface area of particles (coarsening) with increased shearing playing an important role on the microstructure modification. The primary phase grains in the microstructure have two distinct sizes. The larger grains have formed during initial cooling and subsequent isothermal shearing in the semisolid state in the ACME device and the finer grains are presumed to have solidified from the remnant liquid (secondary solidification) following shearing. The strong fluid flow results in melt temperature and composition homogenisation. It also helps dispersing the solute

rejected at the solid-liquid interface reducing constitutional undercooling and its destabilising effect on the solid morphology. Stability of a non-purturbed solid-liquid interface is enhanced under these conditions leading to more compact solid morphologies in contrast to open dendritic structures. Accordingly, the particle morphology observed under shearing shows coarsened dendritic, rosette and globular particles with an increase in shearing time and reduction in shearing temperature. The combined effect of increased substrate wetting and particle coarsening effect of shearing has promoted formation of more globular grains as compared to long dendrites without shear.

The morphology of a single solid particle growing from a binary melt with and without fluid flow has been studied using Monte Carlo simulation [3], as shown in Fig. 7.

Fig. 7a demonstrates that without fluid flow the particle morphology evolves as dendrite with well-defined primary and secondary arms, while coarsening of the dendrite arms leading to a rosette-type structure is observed (

Fig. 7b) when a laminar type unidirectional fluid flow is imposed along with particle rotation,. If fluid flow is introduced in all directions, as expected under high shear rate and turbulence [24], a compact solid morphology evolves as shown in

Fig. 7c. The solute atoms in the melt are represented in grey. As evidenced in

Fig. 7a, thick grey areas of solute-rich regions are evident at the solid-liquid interface and in between dendritic arms. Under fluid flow, the accumulated solute at the solid-liquid interface is dispersed as evidenced from the reduced grey areas in

Fig. 7b. The effect is further enhanced under turbulent type flow in

Fig. 7c where the segregation of grey rejected solute atoms at the solid-liquid interface is minimal. The results corroborate the destabilising effect of solute segregation at the solid-

liquid interface leading to dendritic growth while dispersion of such solutal boundary layer under shearing promotes compact solid morphology through reduction in solid surface area.

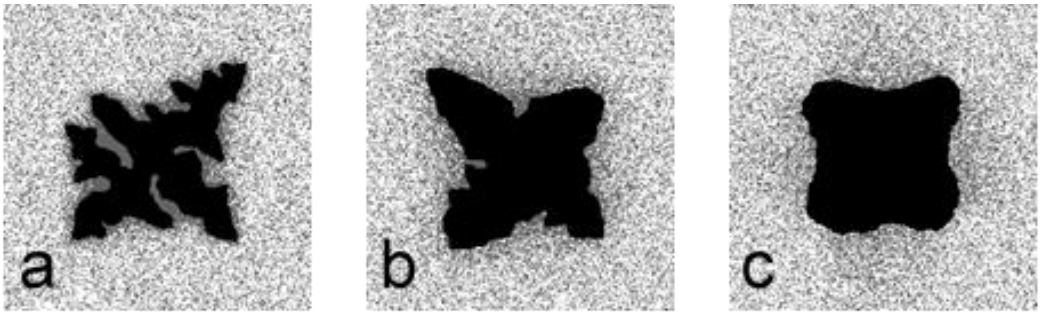

Fig. 7. Growth morphology of solid particle suspended in the melt as simulated through Monte Carlo simulation [3] (a) solid growing in a quiet melt purely under diffusive mass transfer, (b) growth of solid under (laminar-type) unidirectional melt flow from left to right and (c) solid growth under (turbulent-type) flow from both horizontal and vertical directions.

It is difficult to interpret the effect of shear on the microstructural characteristics of equiaxed and refined secondary solidification product. A detailed and systematic investigation into this area is necessary to formulate a universally acceptable explanation. During the secondary solidification after shearing, solid fraction of the primary phase further increases either from growth of the existing grains or through fresh nucleation of the primary phase. Considering the large number of extremely small β– Sn grains observed in the microstructure, it appears that fresh nucleation is prevalent during secondary solidification. In addition, the larger compact primary particles show relatively smooth surfaces indicating minimal growth of existing particles during secondary solidification as such growth is likely to destabilise the compact morphology of the particles. The high shear rate and intense turbulence in the ACME device will create a uniform temperature and solute distribution throughout the semisolid slurry. The remnant liquid is also at its liquidus temperature following shearing. It appears that further growth of the compact primary solid contributes less to the secondary

solid formation as re-establishment of the solutal boundary layer leading to dendritic evolution of particles is sluggish. The remnant liquid may quickly undercool during casting of the semisolid slurry following shearing (secondary solidification) and fresh nucleation (and growth of any particle fragments) is kinetically favoured. The mould surface provides nucleation sites and the undercooling of the bulk remnant liquid would allow survival of nuclei stripped from the mould wall during casting. This may explain the observed fine equiaxed secondary solidification microstructure. This is similar to low-superheat casting that is known to refine microstructure but is more effective due to the temperature homogenisation of the melt from shearing.

The compact particle morphologies formed through shearing (primary solidification) and subsequent casting (secondary solidification) may be gradually lost and revert to dendritic morphology if the semisolid slurry is rested after shearing prior to casting. This is caused by the re-occurrence of local temperature fluctuation and solutal diffusion layer in the melt and promote dendritic growth from the existing primary solid. Therefore, a carefully chosen shearing condition comprising maximum shear rate and time with low resting period prior to subsequent solidification would ensure high number of spherical particles in the final microstructure. It should be noted that the complete potential of shearing will be achieved if the melt is cast immediately after the treatment. Our results also suggest that the primary benefit of shearing comes from thermal and solutal homogenisation of the melt. This ensures survival of nuclei (and fragments) and, most importantly increase the stability, of solid-liquid interface leading to compact particle morphologies. The benefit on secondary solidification also appears to originate from the melt homogenisation effect enhancing secondary nucleation. Large volume of solid nucleation during secondary solidification ensures both refined and non-dendritic microstructure.

Unlike primary β – Sn, the eutectic solidification occurs last in the melt well beyond the withdrawal of shearing. It is, therefore, difficult to comprehend the effect of shearing on the observed eutectic morphology. It is presumed that the difference in eutectic distribution in the absence and presence of shearing doesn't come directly from shearing but as a secondary effect of non-dendritic primary grain formation under shearing. In the absence of shearing, large dendrites have formed in the microstructure. The distribution of remaining liquid in these inter-dendritic pockets are discrete and inhomogeneous. The formation of spherical particles under shear has allowed more even distribution of the remnant liquid in the intergranular areas. Accordingly, the eutectic formed in the microstructure are less clustered and more uniformly distributed over the whole microstructure in the sheared sample.

Effect of shearing on the distribution of Al-rich phase in immiscible alloy

Compared to liquid phase segregation under conventional solidification, intensive shearing using ACME unit in this study has proved effective in dispersing and refining constituent phases in the solidification microstructure of the immiscible alloy. In the Sn-Bi-Al system investigated, Al-rich and Sn-rich liquids form leading to severe segregation in the ingot. The coagulation of individual Sn-rich (L′) and Al-rich (L′′) liquid droplets is driven by surface tension to reduce the overall surface energy. By this mechanism, large droplets grow absorbing smaller ones and small droplets collide amongst themselves to from a single droplet. Droplet motion drives this coagulation and growth of liquid droplets during solidification. Settling of the denser Sn droplets towards the bottom of the mould under gravitational forces can be described by the Stokes motion (U_s) [25]. For a droplet of radius r

$$U_s = \frac{2g\Delta\rho(\eta+\eta')}{3\eta(2\eta+3\eta')}r^2, \quad (1)$$

where, η and η' are the respective viscosities of the liquid matrix and droplets, $\Delta\rho$ is the density difference between the two liquid, and g is the acceleration due to gravity. Even if Stokes motion is minimised, such as in microgravity environment, Marangoni motion (U_m) contributes to the coagulation of liquid droplets from low to high temperature regions [25].This is expressed by:

$$U_m = \frac{2|dT/dx||d\sigma/dT|\kappa}{(2\eta+3\eta')(2\kappa+\kappa')}r, \quad (2)$$

where $d\sigma/dT$is the variation in the interfacial energy between the two liquid phases with a change in temperature, dT/dx is the temperature gradient, and κ and κ' are the thermal conductivities of the liquid matrix and droplets, respectively.

The tendency of the heavier phase (Sn) to segregate at the bottom and the lighter phase (Al) at the top of the conventionally cast immiscible alloy ingot can be attributed to the combined effects of Stokes and Marangoni motions. In the present experiment, the liquid was sheared all the way from above the critical temperature (above the T_c), where a single liquid (L) exists to just below the monotectic temperature (T_m). Intensive shearing and powerful dispersive mixing action in the ACME device promotes the formation of fine liquid droplets both by rupturing the droplets and preventing coagulation from Stokes and Marangoni motion. This is a result of the dynamic equilibrium between two opposite processes, coagulation and breakup of liquid droplets. Inside the ACME unit, the slurry flow direction is against the surface of the blade and stator passages. This produces shear opposite to the direction of the fluid velocity, and the turbulence accelerates the rupturing of droplets and promotes round shape of droplets. The continued shearing from the single liquid to the separated liquids leads to fine and uniformly distributed Al particles in Sn matrix. The final size of liquid droplets (and Al-particles) is dependent on the intensity of the shear and the thermophysical properties of the system, such as interfacial tension and viscosity. In order to counterbalance the force of

gravity, the force was kept high enough, which was achieved by carefully choosing the processing temperature. This is because the viscosity of the melt increases exponentially with the volume fraction of the solid phase and decreases dramatically with an increase in the shear rate and shear time.

Advantages of the ACME unit

The ACME device delivers semi solid material ready for shaping operations. The formable semi solid material allows one-step liquid to near net-shape production. This may be used advantageously to eliminate some of the subsequent thermomechanical processing steps. Advantages over solid-state forming include reduced forming force, high formability and shortened manufacturing time. Compared to melt casting it offers reduced porosity and shrinkage along with benefits from non-dendritic and homogeneous microstructure.

Concluding remarks

Solidification microstructure of Sn-Bi and Sn-Bi-Al alloys formed under intensive shearing has been examined and compare against identical conventional solidification conditions. The present result shown modification of primary β – Sn and distribution of eutectic and Al phase under intensive shearing.

(1) The experimental results from Sn-Bi alloy shows significant microstructure modification by converting well-developed dendritic microstructure to globular primary β – Sn grain and uniformly dispersed Bi-eutectic.

(2) In Sn-Bi-Al immiscible alloys, homogeneous distribution of refined Al-rich particles was retained within the Sn-matrix as opposed to severe segregation observed under conventional solidification.

(3) Shearing temperature and time were noted to influence microstructural refinement. However, the effect of temperature was more dominant than the shearing time. In the immiscible alloy system, shearing was only effective if it started well above the critical temperature and continued into the liquid separation. The effect of shearing on the microstructure modification deteriorated on melt holding following shearing.

ACKNOWLEDGMENT

This research was funded by the Advanced Propulsion Centre (APC), UK for feasibility study. In addition to that, the characterisation facility is supported from the Higher Education Funding Council for England (HEFCE) fund and the WMG Centre High Value Manufacturing Catapult is gratefully acknowledged.

References

[1] M.C. Flemings, Solidification Processing, Materials Science and Technology, Wiley-VCH Verlag GmbH & Co. KGaA2006.
[2] J. Davis, ASM Specialty Handbook: Aluminum and Aluminum Alloys, ASM International (1993).
[3] A. Das, S. Ji, Z. Fan, Morphological development of solidification structures under forced fluid flow: a Monte-Carlo simulation, Acta Materialia 50(18) (2002) 4571-4585.
[4] B.S. Murty, S.A. Kori, M. Chakraborty, Grain refinement of aluminium and its alloys by heterogeneous nucleation and alloying, International Materials Reviews 47(1) (2002) 3-29.
[5] D.H. StJohn, M. Qian, M.A. Easton, P. Cao, Z. Hildebrand, Grain refinement of magnesium alloys, Metallurgical and Materials Transactions A 36(7) (2005) 1669-1679.
[6] G.I. Eskin, D.G. Eskin, Ultrasonic treatment of light alloys metals, 2nd Edition CRS Press (2014).
[7] H.R. Kotadia, M. Qian, D.G. Eskin, A. Das, On the microstructural refinement in commercial purity Al and Al-10wt% Cu alloy under ultrasonication during solidification, Materials & Design 132(Supplement C) (2017) 266-274.
[8] H.R. Kotadia, A. Das, Modification of solidification microstructure in hypo- and hyper-eutectic Al–Si alloys under high-intensity ultrasonic irradiation, Journal of Alloys and Compounds 620(Supplement C) (2015) 1-4.
[9] T.V. Atamanenko, D.G. Eskin, L. Zhang, L. Katgerman, Criteria of Grain Refinement Induced by Ultrasonic Melt Treatment of Aluminum Alloys Containing Zr and Ti, Metallurgical and Materials Transactions A 41(8) (2010) 2056-2066.
[10] C. Vives, Electromagnetic refining of aluminum alloys by the CREM process: Part I. Working principle and metallurgical results, Metallurgical Transactions B 20(5) (1989) 623-629.
[11] Z. Fan, Semisolid metal processing, International Materials Reviews 47(2) (2002) 49-85.
[12] H.R. Kotadia, N. Hari Babu, H. Zhang, Z. Fan, Microstructural refinement of Al–10.2%Si alloy by intensive shearing, Materials Letters 64(6) (2010) 671-673.
[13] H.R. Kotadia, E. Doernberg, J.B. Patel, Z. Fan, R. Schmid-Fetzer, Solidification of Al-Sn-Cu Based Immiscible Alloys under Intense Shearing, Metallurgical and Materials Transactions A 40(9) (2009) 2202-2211.
[14] M. Qian, A. Das, Grain refinement of magnesium alloys by zirconium: Formation of equiaxed grains, Scripta Materialia 54(5) (2006) 881-886.
[15] Z. Fan, Y. Wang, M. Xia, S. Arumuganathar, Enhanced heterogeneous nucleation in AZ91D alloy by intensive melt shearing, Acta Materialia 57(16) (2009) 4891-4901.
[16] A. Das, H.R. Kotadia, Effect of high-intensity ultrasonic irradiation on the modification of solidification microstructure in a Si-rich hypoeutectic Al–Si alloy, Materials Chemistry and Physics 125(3) (2011) 853-859.
[17] M.C. Flemings, Behavior of metal alloys in the semisolid state, Metallurgical Transactions B 22(3) (1991) 269-293.
[18] Z. Cassinath, International patent application number PCT/GB2015/052409. (2016).
[19] Z. Cassinath, A.K. Prasada Rao, Development of Axial Continuous Metal Expeller for melt conditioning of alloys IOP Conf. Series: Materials Science and Engineering (114 (2016) 012042) (2016).
[20] A.M. Mullis, Growth induced dendritic bending and rosette formation during solidification in a shearing flow, Acta Materialia 47(6) (1999) 1783-1789.
[21] H.R. Kotadia, A. Das, E. Doernberg, R. Schmid-Fetzer, A comparative study of ternary Al–Sn–Cu immiscible alloys prepared by conventional casting and casting under high-intensity ultrasonic irradiation, Materials Chemistry and Physics 131(1) (2011) 241-249.
[22] A. Das, G. Liu, Z. Fan, Investigation on the microstructural refinement of an Mg–6wt.% Zn alloy, Materials Science and Engineering: A 419(1) (2006) 349-356.
[23] H.R. Kotadia, J.B. Patel, H.T. Li, F. Gao, Z. Fan, Microstructure Evolution in Melt Conditioned Direct Chill (MC-DC) Casting of Fe-Rich Al-Alloy, Advanced Materials Research 1019 (2014) 90-95.

[24] A. Das, Z. Fan, Morphological development of solidification structures under forced fluid flow: experimental observation, Materials Science and Technology 19(5) (2003) 573-580.
[25] M. Lappa, Fluids, Materials, and Microgravity 1st Edition (Numerical Techniques and Insights into Physics), Elsevier Science., Oxford (2004).